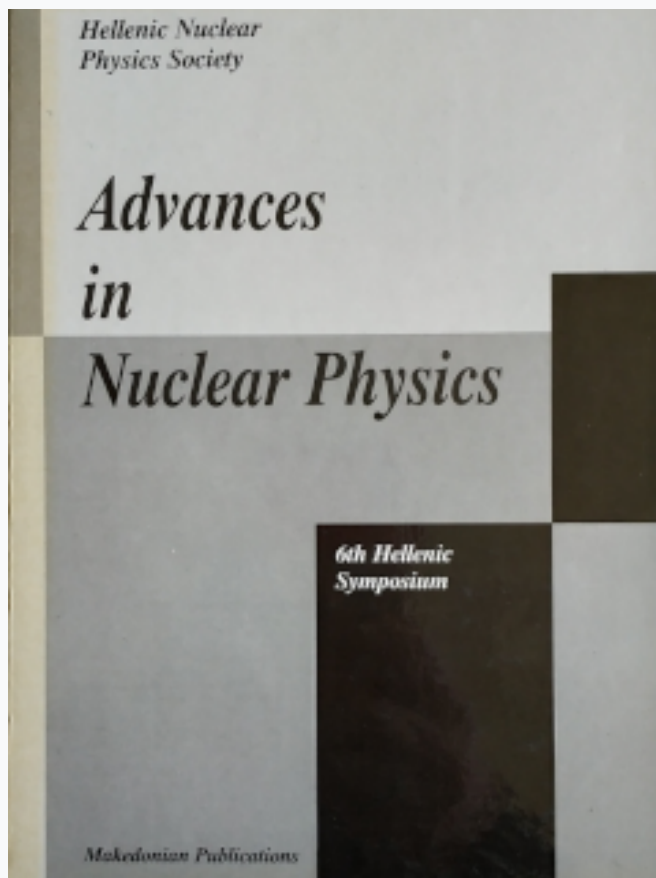


## HNPS Advances in Nuclear Physics

Vol 6 (1995)

HNPS1995



### The Compton electron beam Polarimeter for the AmPS ring

*N. P. Vodinas, C. W. de Jager, N. H. Papadakis, I. Passchier*

doi: [10.12681/hnps.2941](https://doi.org/10.12681/hnps.2941)

#### To cite this article:

Vodinas, N. P., de Jager, C. W., Papadakis, N. H., & Passchier, I. (2020). The Compton electron beam Polarimeter for the AmPS ring. *HNPS Advances in Nuclear Physics*, 6, 338–349. <https://doi.org/10.12681/hnps.2941>

# The Compton electron beam polarimeter for the *AmPS* ring

N.P. Vodinas <sup>a,1</sup>, C.W. de Jager <sup>a</sup>, N.H. Papadakis <sup>a,1</sup> and I. Passchier <sup>a</sup>

<sup>a</sup> *NIKHEF/FOM P.O.Box 41882, 1009 DB Amsterdam, The Netherlands*

---

## Abstract

The longitudinal polarization of the stored electron beam in the *AmPS* ring will be measured through the laser Compton backscattering technique. With the outlined design the measurement of the expected 70% degree of polarization to a statistical precision of 3% requires less than 60 sec under ideal conditions.

---

## 1 Introduction

The continuous beam electron facilities, that are becoming operational worldwide, form an excellent tool for research in nuclear and hadronic physics with electromagnetic probes. The use of polarized electrons and polarized targets is considered an essential factor in their experimental programs [1].

A design for producing an intense stored beam of longitudinally polarized electrons at the Interaction Point (*IP*) of the existing Internal Target Hall (*ITH*) of the *MEA/AmPS* facility has been made by a collaboration between *NIKHEF* and the *BINP* and *ISP* Institutes from Novosibirsk. Technically the polarization project comprises of the construction of a polarized electron injector and a Siberian Snake to compensate the depolarization effects in the ring [2], [3]. A beam polarimeter, based on the laser Compton backscattering technique, has been designed and installed in the *AmPS* ring for measuring and monitoring continuously the longitudinal polarization of the stored electron beam.

---

<sup>1</sup> present address: IASA, Division of Accelerating Physics, P.O.Box 17214, 10024 Athens, Greece

The spin-dependent Compton scattering of circularly polarized photons off polarized electrons is currently used or planned as a fast, non-destructive, and accurate method for measuring the polarization of high-energy electron beams in storage rings at different laboratories [4].

In the following sections the physics of the Compton scattering is briefly discussed and the main features of the design of the laser Compton backscattering beam polarimeter for the *AmPS* ring are presented.

## 2 The Physics of the Compton Scattering

The Compton effect involves the scattering of energetic photons off free (or quasi-free) electrons. If photons with energy  $E_\lambda$  in the *LAB* frame collide head-on with electrons of energy  $E_e$  and velocity  $\beta$ , the energy  $E_\gamma$  of the scattered photons is given by

$$E_\gamma = \frac{(1 + \beta)E_\lambda}{1 - \beta \cos\theta_\gamma + \frac{E_\lambda}{E_e}(1 + \cos\theta_\gamma)} \quad (1)$$

where  $\theta_\gamma$  is the angle of scattered photons with respect to the incident electrons. For high electron beam energies and for incoming photons with energy corresponding to typical laser systems the most energetic photons are emitted into a narrow cone centered on the direction of the incoming electron beam. The maximum energy of scattered photons,  $E_\gamma^{max}$ , occurs for  $\theta_\gamma = 0^\circ$  independently of the energy of the incoming electron and photon beams.

In the *LAB* frame the differential cross section for Compton scattering of circularly polarized photons off longitudinally polarized electrons can be expressed as [5]

$$\frac{d\sigma}{dE_\gamma} = \frac{d\sigma_0}{dE_\gamma} [1 + S_3 P_Z \alpha_{3z}(E_\gamma)] \quad (2)$$

where  $\frac{d\sigma_0}{dE_\gamma}$  is the differential cross section for unpolarized Compton scattering,  $P_Z$  is the degree of longitudinal polarization of the electron beam and  $S_3$  is the Stokes parameter that defines the circular polarization of the incident photon beam;  $S_3 = +1(-1)$  for completely left (right)-handed polarized photons. The quantity  $\alpha_{3z}$  is the longitudinal analysing strength. The analysing strength depends on the energy of the electron and photon beams. For a given electron energy the shorter the laser wavelength the larger the analysing strength. In addition more energetic electron beams result in larger analysing strengths in polarized Compton scattering.

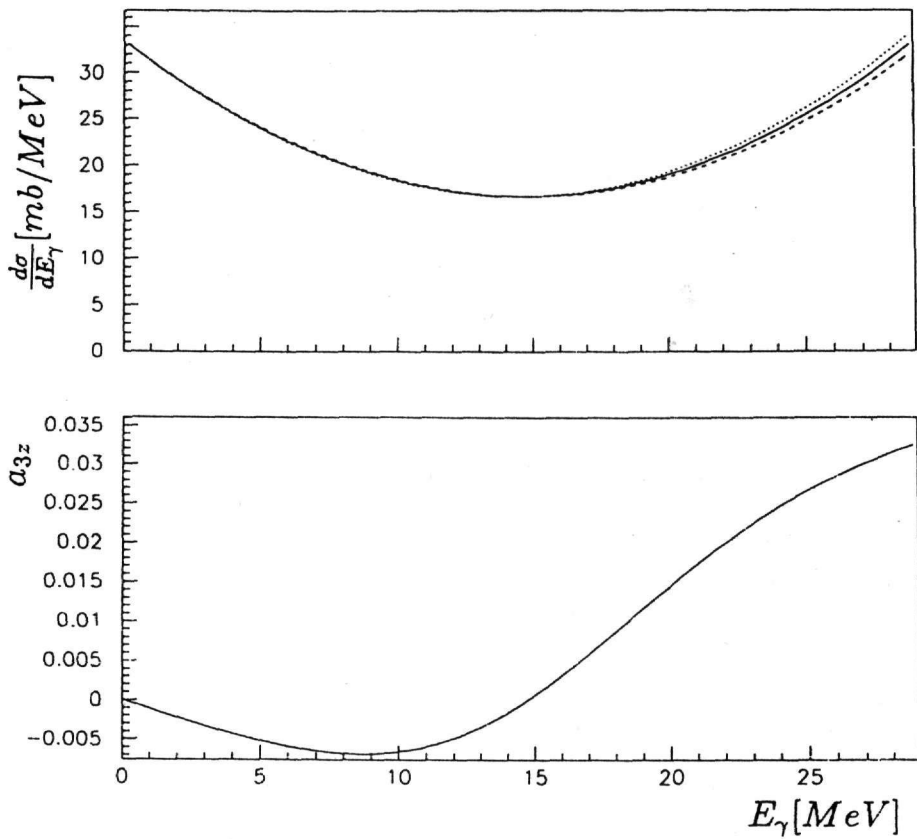


Fig. 1. The energy spectra of backscattered photons (top) and the longitudinal analysing strength  $a_{3z}$  (bottom) in Compton scattering.

The energy spectra and the longitudinal analysing strength in Compton scattering are presented in Figure 1 for an energy of  $E_e = 900 \text{ MeV}$  and for laser photons with an energy of  $E_\lambda = 2.41 \text{ eV}$  that corresponds to a wavelength of  $\lambda = 514.5 \text{ nm}$ . Solid lines in Figure 1(top) represent the unpolarized case. For comparison the energy spectra of the polarized Compton scattering are plotted for the cases of  $S_3 P_Z = +1$  (dotted lines) and  $S_3 P_Z = -1$  (dashed lines). In Figure 1(bottom) the quantity  $\alpha_{3z}$  is plotted as a function of the energy of backscattered photons. Larger longitudinal analysing strengths correspond to backscattered photons with higher energies. The maximum value of the longitudinal analysing strength occurs for backscattered photons with energy  $E_\gamma^{max}$ .

### 3 The Measurement of the Longitudinal Polarization

If a circularly polarized photon beam is backscattered off the electron beam, the scattered intensity will depend on the helicity of the light and the electron spin according to the Compton cross section. By switching the helicity of the light and/or the electron the resulting asymmetries can provide a direct measurement of the electron beam polarization.

The experimental asymmetry in the counting rate for Compton scattering,  $A_C$ , is given by

$$A_C = \frac{N_R - N_L}{N_R + N_L - 2N_{bkgd}} \quad (3)$$

where  $N_R$  and  $N_L$  are the total number of backscattered photons normalized to the integrated beam current for right and left helicities of the incident photons respectively.  $N_{bkgd}$  represents the background contribution. The quantity  $A_C$  is related to the longitudinal electron polarization  $P_Z$  via the following relation

$$P_Z = \frac{A_C}{S_3 \langle \alpha_{3z} \rangle} \quad (4)$$

The average analysing strength  $\langle \alpha_{3z} \rangle$  is calculated in the kinematical region defined by the angular acceptance of the detector.

The total number of backscattered photons,  $N_\gamma$ , for right and left helicities of the initial photons, is related to the relative accuracy of the longitudinal asymmetry (polarization)  $\frac{\Delta A_C}{A_C} \left( \frac{\Delta P_Z}{P_Z} \right)$  via

$$\frac{\Delta A_C}{A_C} = \frac{\Delta P_Z}{P_Z} = \sqrt{\frac{1 - A_C^2}{N_\gamma A_C^2}} \quad (5)$$

where the error of  $S_3$  has been neglected.

The required total measuring acquisition time,  $T(sec)$ , as a function of the beam polarization  $P_z$  for a given relative accuracy can be expressed as

$$T = \frac{N_\gamma}{\dot{N}_\gamma} = \frac{1 - (S_3 P_z < a_{3z} >)^2}{(S_3 P_z < a_{3z} >)^2 \left(\frac{\Delta P_z}{P_z}\right)^2 \dot{N}_\gamma} \quad (6)$$

where  $\dot{N}_\gamma(Hz)$  is the count rate of backscattered Compton photons. In the case of continuous electron and laser beams the rate of backscattered Compton photons can be estimated from

$$\dot{N}_\gamma = 2\dot{N}_{ph} \frac{N_e L}{C} \frac{1}{\Sigma} \sigma_{C0} \quad (7)$$

where,  $\dot{N}_{ph}(photons/sec)$  is the initial photon flux,  $N_e$  is the number of electrons circulating in the ring,  $C(m)$  is the circumference of the storage ring,  $L(m)$  is the length of the Interaction Region (*IR*) of the electron beam with the laser light,  $\Sigma(cm^2)$  is the larger of the transverse sizes of the electron and the laser beam, and  $\sigma_{C0}(cm^2)$  is total the cross section for unpolarized Compton scattering.

## 4 The Beam Polarimeter of *AmPS* ring

### 4.1 The layout

A schematic layout of the Compton polarimeter with its position in the *AmPS* ring is shown in Figure 2 [6]. The polarimeter consists of the laser system with its associated optical system and a detector for the detection of backscattered photons. The straight section ( $\sim 2.5 m$ ) between the first two dipoles after the Internal Target Facility (*ITF*) has been chosen as the electron beam-laser light *IR*. The crossing angle between the laser and the electron beams should be as small as possible in order to maximize the luminosity of the interaction. Another criterion, for the choice of the *IR*, is that the backscattered photons should be separated from the large bremsstrahlung background coming out from the 32 m long *West* straight section of *AmPS*. The backscattered photons leave the *IR* traveling in the same direction as the electrons of the beam and are separated after the second dipole.

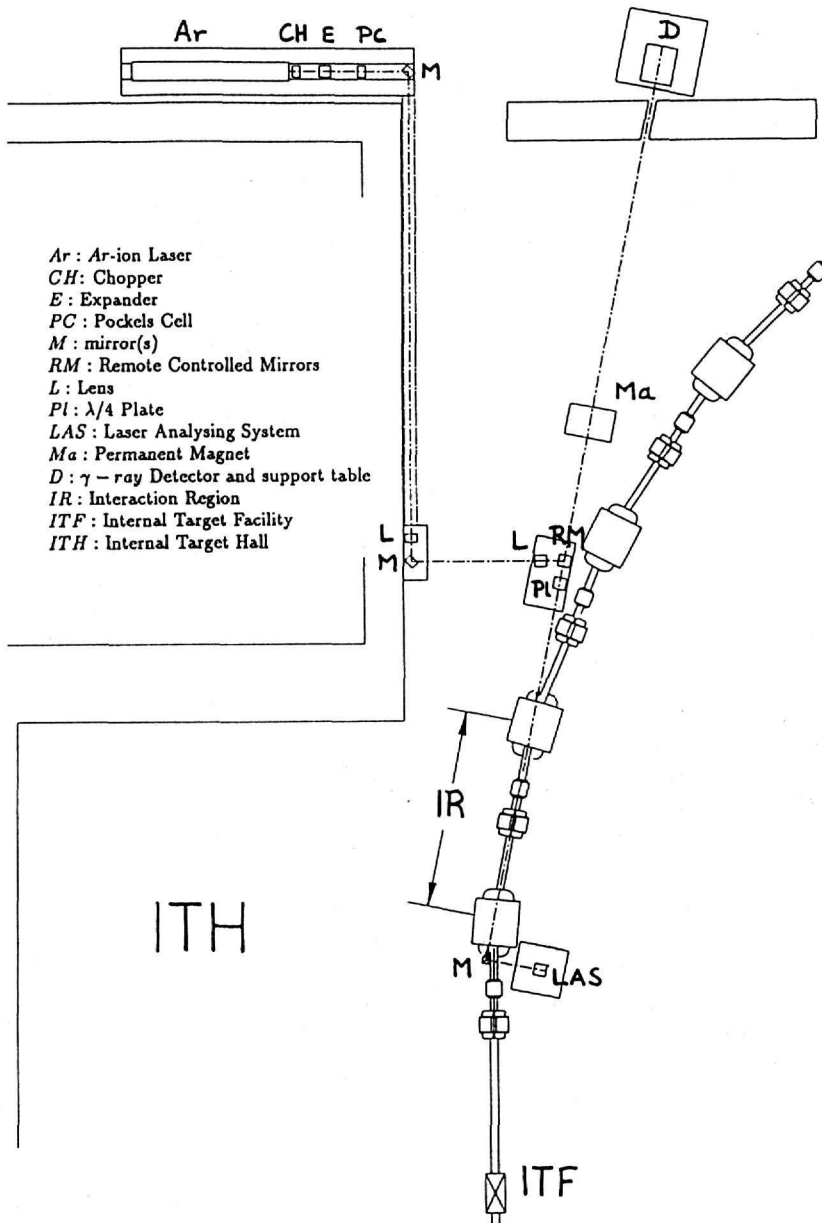


Fig. 2. Schematic layout of the electron beam polarimeter for the AmPS ring.

## 4.2 The laser and the associated optical system

An Ar-ion laser system has been selected, which can provide a 10 W continuous  $TEM_{00}$ -mode beam at  $\lambda = 514.5$  nm with a divergence of 0.4 mrad (full angle) and diameter of 1.8 mm.

The laser light is guided to the IR, over a total path of approximately 12 m, by a system of mirrors and lenses entering the IR through a 25 mm diameter sapphire vacuum window. Circularly polarized light is generated by the combined use of a Pockels Cell (PC) and an anti-reflection coated quarter-wave ( $\lambda/4$ ) plate (PI). Left-handed and right-handed polarized light is obtained by switching the high voltage on the PC. In order to minimize the degradation of the polarization during the transport of the laser light to the IR by reflections off the mirrors, the use of the PC as a half-wave ( $\lambda/2$ ) plate is decided. The scheme of transporting either vertical or horizontal light and transforming it into circular polarized light using the  $\lambda/4$  plate positioned before the entrance window to the IR is adopted. In order to prevent both the Ar-ion laser and the PC from radiation damage they will be installed at the niche of NW area of the AmPS ring placed on a specially designed support structure. A chopper (CH) is mounted on the laser support structure to block the beam for background measurements.

The first fixed mirror ( $M_1$ ) deflects the laser light by  $90^\circ$  and is used to steer it along the wall, in the direction of the ITH. Another deflection of  $90^\circ$  from a fixed second mirror ( $M_2$ ) directs the laser beam into a system of three mirrors (RM) consisting of two remote controlled mirrors and a third fixed mirror. This system of mirrors will be used to scan the electron beam in horizontal and vertical direction both in position and in angle. The first remote controlled mirror can be tilted in both angles and is connected to a translation stage. The laser beam leaving this mirror can be translated in one direction (horizontal) and can scan in both angles. The second remote controlled mirror is positioned in a second translation stage, producing the vertical translation of the laser beam. The laser beam leaves this mirror pointing in the vertical direction and deflects the laser light to the last mirror before the IR. This last fixed mirror is used to guide the laser light to the IR. All mirrors having diameter of 50 mm are dielectric mirrors optimized for  $45^\circ$  incidence for both 514.5 nm and 488 nm wavelengths. Mounts of fixed mirrors are adjusted by hand. DC motors are chosen for the mounts and translation stages of the remote controlled mirrors.

To facilitate the transport of the laser beam and in order to prevent the PC from high power damages a Galilean expander (E) consisting of two lenses with focal lengths of  $f_1 = -2.5$  cm and  $f_2 = 8.0$  cm is used before the PC. The lenses of the expander are located on the laser support structure with



coinciding focal points on the optical axis to obtain an almost parallel beam leaving the expander. The laser beam is focussed at the *IR* by the system of two lenses  $L_3$  and  $L_4$  with focal lengths of  $f_3 = 200\text{ cm}$  and  $f_4 = 76\text{ cm}$  respectively. The size of the beam at the *IR* can be changed by adjusting the position of lens  $L_3$ . All lenses are diffraction limited lenses and have anti-reflection coatings for both  $514.5\text{ nm}$  and  $488\text{ nm}$  wavelengths.

After the interaction with the electron beam the laser photons exit the *IR* through a second  $25\text{ mm}$  diameter sapphire window to a pair of locally phase-compensated dielectric fixed mirrors ( $M_3$ ) with diameter of  $50\text{ mm}$ . This pair of mirrors is used to deflect the laser light first downward and then sideways underneath the beam pipe of *AmPS* to an analysing system consisting of a rotating Glan-Thompson prism and a power-meter.

The small fraction of the laser light transmitted through the mirrors is utilized to measure the size and monitor the position of the laser beam using *VIDICON* camera's located before and after the *IR*.

#### 4.3 Detector and background considerations

The detector ( $D$ ) of the backscattered photons will be situated  $\sim 10 - 12\text{ m}$  downstream of the *IR* and should be capable of detecting  $\gamma$ -rays of up to  $30\text{ MeV}$ , handling count rates of the order of few hundred of  $\text{kHz}$  and be radiation resistant. Total absorption shower counters made of dense inorganic scintillating crystals are possible candidates [7]. The use of scintillating crystals made of  $\text{BaF}_2$  (fast component),  $\text{CsI}$  (undoped) and  $\text{CeF}_3$  is investigated. Dense crystals with shorter radiation length and Moliere radius offer smaller detector volume.

At the beginning and in order to test and tune our optical system the use of a composite  $\gamma$ -ray spectrometer is decided [8]. The main detector of this spectrometer is a cylindrical *BGO* scintillator crystal ( $102\text{ mm}$  diameter and  $100\text{ mm}$  long), canned in an aluminum box  $0.8\text{ mm}$  thick, optically coupled to a Hamamatsu *R1250* photomultiplier. The crystal is surrounded by plastic (*NE110*) cylindrical scintillator shell divided in three  $120^\circ$  sectors optically separated by an aluminum foil,  $0.8\text{ mm}$  thick, each one seen by two *XP2312B* photomultipliers, encased in an aluminum cylinder,  $325\text{ mm}$  long,  $420\text{ mm}$  external diameter and  $120\text{ mm}$  internal diameter. This plastic scintillator shell will be used in anti-coincidence mode as a Compton suppression shield. A plastic scintillator in the front of this spectrometer will be used as the veto for the charged particles background.

Several sources of background have to be considered; sources of background photons produced by the electron beam are the synchrotron radiation and the

bremstrahlung from the rest-gas molecules in the beam pipe. Off-momentum electrons produced by bremstrahlung of beam particles with rest-gas molecules are the dominant source of the high energy electron background.

The main sources of synchrotron radiation in the line of sight of the detector are the two dipoles before and after the *IR* with bending radius of  $\rho = 3.30\text{ m}$ . For these dipoles the rate of synchrotron photons with energies above  $\epsilon = 100\text{ keV}$  for  $900\text{ MeV}$  beam energy is completely negligible. Since only photons with energy of the order of several  $\text{MeV}$  are required for the asymmetry, the synchrotron photons can be filtered out effectively with some high  $Z$  mask (copper, lead or tungsten).

Assuming a  $N_2$  residual gas at room temperature and path length of  $l_t = 300\text{ cm}$ , gas bremstrahlung calculations indicate that in order to avoid problems with the dead-time of the detector and for a signal-to-background ratio of the order of 10 times the pressure of the residual gas should be maintained lower than  $10^{-8}\text{ Torr}$ . Photons produced by bremstrahlung can be measured by blocking the laser light with the Chopper and can be subtracted from the data.

A major part of the electron background can be deflected by using a sweeping magnet (*Ma*) in the line of sight of the detector followed collimators (not shown in the layout) that can collimate away any electrons passing the magnet.

#### 4.4 *The expected measuring time*

Detailed simulations based on Monte Carlo techniques (*GEANT*) have been performed in order to study the Compton process and evaluate the expected measuring time for the longitudinal polarization, taking into account the electron beam phase space and the laser beam behaviour along the *IR*. Typical values of the Twiss parameters at the center of the *IR* used for the simulations are  $\alpha_x = -1.31$ ,  $\beta_x = 2.7\text{ m}$  and  $\alpha_y = 1.95$ ,  $\beta_y = 7.91\text{ m}$ . The horizontal and vertical emittances for a  $900\text{ MeV}$  energy are  $\epsilon_x = 1.28 \times 10^{-7}\text{ rad}\cdot\text{m}$  and  $\epsilon_y = 0.32 \times 10^{-7}\text{ rad}\cdot\text{m}$  respectively [9]. For a circulating electron beam with energy of  $E_e = 900\text{ MeV}$  and current  $I = 75$  the simulations show that the time required for the measurement of a longitudinal beam polarization of  $P_Z = 0.7$  with a statistical precision of  $\Delta P_Z/P_Z = 3\%$  is less than  $60\text{ sec}$ . In the calculations a totally circularly polarized laser beam ( $S_3 = 1$ ) with spot diameter equal to  $2.25\text{ mm}$ , originating from a  $10\text{ W Ar-ion}$  laser and operating at  $\lambda = 514.5\text{ nm}$ , is used. The *IR* of the electron and laser beams is assumed to be  $1\text{ m}$  long.

#### 4.5 The Control and Data Acquisition System

The control of the polarimeter will be performed with a computer code developed with LabVIEW on a *SUN*-workstation (see Figure 3). The control of the laser and the laser beam will be done via a *GP*IB card, which is connected to the workstation via Ethernet. The four DC-motors used for the steering of the laser beam are controlled by an *PI804* motor controller from Physik Instrumente. A resolution of  $2\ \mu\text{m}$  and  $60\ \mu\text{rad}$  can be obtained with the *PI804* and the DC-motors. The *PI804* has also four analog inputs, of which one will be used to read out the power-meter (*JM*) in the laser analysing system.

The Data Acquisition will be done with a single *VME*-module, designed and constructed at *NIKHEF*. The module has three analog and three digital inputs. One of the analog inputs is used for the detector signals and is connected to an 8-bit flash-*ADC*. The other two analog inputs can be used for the charged particle veto detector (*VETO*) and the Compton Suppression Shield (*CSS*) and are connected to Discriminators. The three digital inputs are used as inhibit, and as messengers about the polarization state of the laser light and whether the laser light is blocked or not by the Chopper. All these digital signals are generated by the Chopper. If none of the Discriminator inputs is above threshold and if no inhibit exists, the *ADC* value is stored. In this way, four histograms are build inside the *VME*-module, representing the energy spectrum of  $\gamma$ -rays in the detector for left and right handed laser light, both with and without laser beam in the *IR*. The maximum rate at which the module can operate is  $\approx 1\ \text{MHz}$ . The module is read out typically every 15 sec via the *SBUS* of the workstation. The conversion from the energy spectra to electron polarization will be done by comparing the measured asymmetry with the results of *GEANT*.

## 5 Summary

The laser backscattering Compton technique for electron polarimetry has been reviewed and a design procedure for a Compton-laser polarimeter for the *AmPS* ring has been presented. The polarimeter consists of a laser system producing circularly polarized light, the laser transport and analysing system and a total absorption photon detector capable of detecting photons with energy up to several tens of MeV. The straight section between the two dipoles of the first curved section after the *ITF* will be used as the electron-laser *IR*. Monte Carlo simulations, for a continuous *Ar*-ion laser with  $\lambda = 514.5\ \text{nm}$  operating at  $10\ \text{W}$ , predict that the measurement of the expected 70% degree of longitudinal polarization of a  $75\ \text{mA}$  circulating electron beam with energy of  $900\ \text{MeV}$  can be achieved, with an accuracy of 3%, in a time less than 60

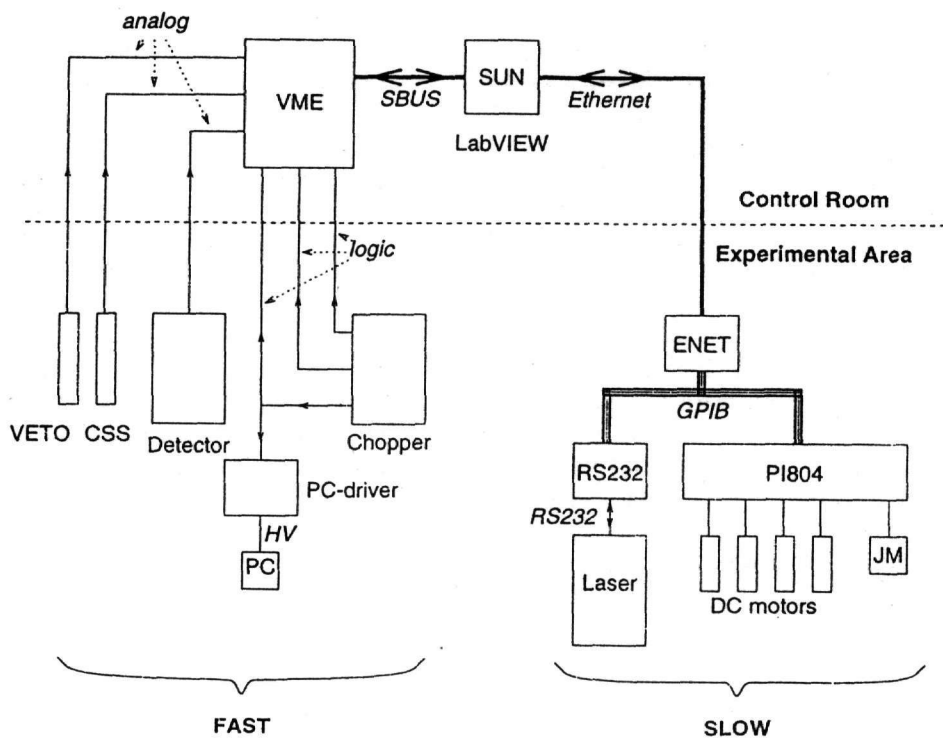


Fig. 3. Schematics of the Control and the Data Acquisition System of the laser Compton backscattering polarimeter.

sec under ideal conditions.

## Acknowledgment

This work is part of the research programme of the Nuclear Physics section of NIKHEF, made possible by financial support from the Stichting voor Fundamenteel Onderzoek der Materie (*FOM*), which is financially supported by the Nederlandse Organisatie voor Wetenschappelijk Onderzoek (*NWO*). Two of the authors, NHP and NPV, are supported by the Human Capital and Mobility programme of the EEC under contracts nr. ERBCHBICT930606 and CHRX-CT93-0122 respectively.

## References

- [1] 11<sup>th</sup> International Symposium on High Energy Physics and 8<sup>th</sup> International Symposium on polarization phenomena in Nuclear Physics, Bloomington Indiana (USA), September 15-22, 1994
- [2] C.W. de Jager, "Spin Physics in the (e,e' p) Reaction off the Deuteron" Spin Physics at Intermediate Energies, Lecture notes of the 1992 RCNP-Kikuchi school, RCNP-P-128, pp.91 Osaka (Japan), 1992
- [3] N.H. Papadakis et al., 'Polarized electrons at *NIKHEF*' Contribution to this Symposium
- [4] (i) L. Knudsen et al., Phys.Lett. B270(1991) 97 (ii) M.J. Fero, Proceedings of the 10<sup>th</sup> International Symposium on High Energy Spin Physics, pp.899, Nagoya (Japan) 1992 (iii) D.P. Barber et al., NIM A329(1993) 79 and NIM A338(1994) 166
- [5] (i) F.W. Lipps and H.A. Tolhoek, Physica 20(1954)85; ibidem 395 (ii) H.A. Tolhoek, Rev.Mod.Phys 28(1956) 277
- [6] N.P. Vodinas, C.W. de Jager, N.H. Papadakis, I. Passchier, Report EMIN 95-03, NIKHEF-K
- [7] G. Gratta, H. Newman, and R.Y. Zhu, Ann.Rev.Nucl.Part.Sci. 45(1994) 453
- [8] P. Corvisiero et al., NIM A294(1990) 478
- [9] Y. Wu, 'The Optical Design of *AmPS*' PhD Thesis, Techn. Univ. of Eindhoven, November 1991 (unpublished)